Comparative Analysis of Neural-Adaptive and Neuro-Sliding Control Strategies for Vibration Attenuation in Flexible Structures

Alejandro Díaz[1], Rita Q. Fuentes-Aguilar[2] and Javier Ruiz-Leon[3]

Abstract— **This work addresses the challenge of active vibration attenuation in flexible structures by proposing an improved control architecture based on Finite Element Differential Neural Networks (FEDNN). Unlike traditional black-box identifiers, the FEDNN incorporates the spatial topology of the Finite Element Method, enabling a physics-consistent approximation of spatiotemporal dynamics. The network is identified offline using experimental data acquired from a cantilever beam, which serves as a canonical distributed parameter system. Based on this data-driven model, two distinct control strategies are synthesized and compared: a nodal Model Reference Adaptive Control (MRAC) and a distributed Neural-Sliding Mode Control (NSMC). Numerical results demonstrate that while both approaches successfully reject persistent non-vanishing disturbances, they exhibit distinct operational characteristics. The study concludes by analyzing the trade-offs between the robustness of the distributed sliding mode approach and the smooth, energy-efficient performance of the proposed nodal MRAC scheme.**

I. INTRODUCTION

Many engineering and control systems are accurately represented by Distributed Parameter Systems (DPS). These systems are mathematically modeled through Partial Differential Equations (PDEs), which are often analytically intractable due to their complexity. Consequently, the use of numerical approximations and Neural Networks (NN) has become increasingly frequent in the analysis and control of such systems.

However, the precise control of DPS, particularly in flexible structures such as manipulators, aircraft wings, and cantilever beams remains a significant challenge due to their infinite-dimensional nature and complex spatio-temporal coupling. In practical applications, these systems are invariably subject to parametric uncertainties and persistent external disturbances. To mitigate these issues, Model Reference Adaptive Control (MRAC) has emerged as a standard solution, designed to ensure robust performance by forcing the plant to track a desired behavior defined by a reference model. The versatility of MRAC is evidenced by its application across diverse fields, ranging from robotics [1] to renewable energy systems [2].

*This work was not supported by any organization

[1]Alejandro Díaz is with Faculty of Electrical Engineering, CINVESTAV, Zapopan 45069, Jalisco, México jesus.diaz@cinvestav.mx

[2]Rita Q. Fuentes-Aguilar with Institute of Advanced Material for Sustainable Manufacturing, Tecnológico de Monterrey, Zapopan, 45069, México rita.fuentes@tec.mx

[3]Javier Ruiz-Leon is with Faculty of Electrical Engineering, CINVESTAV, Zapopan 45069, Jalisco, México javier.ruiz@cinvestav.mx

Despite its popularity, conventional MRAC design faces critical limitations, particularly when applied to flexible structures. A primary challenge lies in the inevitable discrepancy between the mathematical model and the physical plant, often referred to as "model mismatch" [3]. This issue is exacerbated by unmodeled dynamics, material degradation [4], and unforeseen perturbations.

To address the specific problem of disturbance rejection, Variable Structure Control, and specifically Sliding Mode Control (SMC), has established itself as a rigorous alternative [5], [6]. SMC is renowned for its invariance properties to matched perturbations, making it a powerful tool for vibration suppression. However, its practical implementation is often hindered by the "chattering" phenomenon—high frequency control switching that causes actuator wear—and the frequent requirement for distributed sensing and actuation to maintain the sliding manifold [7].

Recent research has sought to enhance both adaptive and robust schemes by integrating Neural Networks (NN). Prominent works, such as [8], have utilized NNs to adjust adaptation laws dynamically. Similarly, studies like [9], [10] and [11] apply reinforcement learning for complex control problems [12], [13], [14]. However, most neuro-adaptive approaches focus primarily on the feedback loop logic [15], often overlooking a fundamental limitation shared by both MRAC and SMC strategies: the selection of the reference model itself.

While some approaches attempt to mitigate saturation or generate trajectories [16],[17], they often lack a rigorous connection to the underlying physical topology. Typically, a low-order linear system (e.g., a standard second-order damped oscillator) is chosen to define the target dynamics. For highly flexible systems, imposing such idealized linear dynamics creates a "reference mismatch", where the requested trajectory (or decay rate) is physically unattainable by the plant given its structural constraints. This often forces the controller to saturate [16], regardless of whether it is an adaptive or sliding mode scheme.

In this work, we propose the utilization of a novel kind of NN, and implemented it in two different control architectures in order to validate its performance. Instead of forcing the beam to mimic an arbitrary linear model, the FEDNN—which approximates the system's full spatio-temporal dynamics based on the Finite Element Method—generates a feasible reference trajectory that respects the nodal connectivity and physical limitations of the system.

Using this "digital shadow" as the reference, we conduct a rigorous comparative analysis between a nodal MRAC with harmonic regressor augmentation and a distributed Neural-Sliding Mode Control (NSMC). The study aims to demonstrate that by addressing the reference mismatch problem via FEDNN, it is possible to achieve vibration suppression performance, and give a final note about the trade-off for practical engineering applications.

The remainder of this work is organized as follows: Section II provides the mathematical description of the system and details the FEDNN implementation. Section III discusses the synthesis of the control strategies enhanced by the neural reference. Numerical validation results are presented in Section IV, and finally, the comparative analysis of the operational trade-offs is provided in Section V.

II. SYSTEM DESCRIPTION AND IDENTIFICATION

A. *Flexible Beam Dynamics*

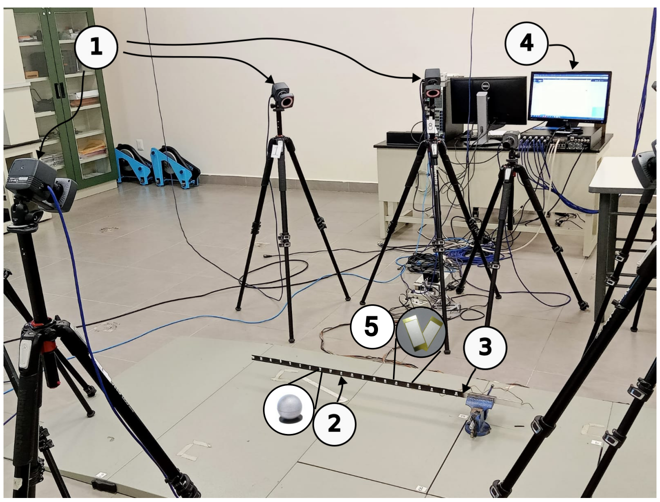

Fig. 1: View of the experimental platform illustrating: (1) MoCap camera system, (2) Installed sensors, (3) Clamped aluminum beam, (4) The host workstation, and (5) PZT actuators.

The experimental platform consists of a flexible aluminum structure configured as a cantilever beam. The beam is instrumented with reflective markers located at the nodes defined by the finite element partition. These markers are tracked by a Motion Capture (MoCap) system, which transmits the real-time position and velocity of each node to the workstation, as shown in Fig. 1.

Unlike approaches such as [18] that utilize the Timoshenko beam theory, this work adopts the Euler-Bernoulli formulation to describe the system's dynamics. Accordingly, the governing Partial Differential Equation (PDE) is defined as:

$$\rho\frac{\partial^2 v(x,t)}{\partial t^2} + \frac{\partial^2}{\partial x^2}\left(EI\frac{\partial^2 v(x,t)}{\partial x^2}\right) = q(x,t) + \xi(x,t) \quad (1)$$

where $v(x,t)$ is the transverse displacement of the beam (m), ρ is the density (kg/m^3) of the beam material, EI is the beam rigidity (N/m), $q(x,t)$ is the externally applied pressure loading (Pa) and $\xi(x,t)$ is the modeling error and the potential effect of external perturbations. We assume that $\xi(x,t)$ is bounded, leading to the following set of admissible uncertainties/perturbations:

$$\Omega = \left\{\xi(x,t)\,\middle|\, \quad \|\xi(x,t)\| \leq \overset{+}{\xi} \quad \forall t \wedge x \in [0,L]\right\} \quad (2)$$

As presented in [19] this system can be represented by FEM modeling as:

$$[M]\{\ddot{d}(t)\} + [K]\{d(t)\} = \{F(t)\} + \{\bar{\xi}(t)\} \quad (3)$$

where $[M] \in \mathbb{R}^{N\times N}$ is the assembled mass matrix, $[K] \in \mathbb{R}^{N\times N}$ is the assembled stiffness matrix, $F(t) \in \mathbb{R}^{N\times m}$, with m representing the number of nodes where a force can be applied, is the force function acting on the beam, and $\bar{\xi}(t) \in \mathbb{R}^{N\times N}$ is the FEM modeling error. The expression of $\{d\}$ is given as the elemental nodal degrees of freedom, that is, $d = \begin{bmatrix} d_1 & d_2 & \cdots & d_N \end{bmatrix}^\top$, where d_i is the displacement of the node in the composition and N is the number of nodes in which the system was divided excluding the fixed node due to boundary conditions.

By reorganizing equation (3), we obtain.

$$\{\ddot{d}(t)\} = [M]^{-1}(\{F(t)\} + \{\bar{\xi}(t)\} - [K]\{d(t)\}). \quad (4)$$

We can utilize a state-space interpretation given as:

$$\begin{aligned} \dot{x}_1(t) &= x_2(t) \\ \dot{x}_2(t) &= f\left(t, x_1(t), x_2(t)\right) + \eta(t) \end{aligned} \quad (5)$$

where $\eta(t) = [M]^{-1}\{\bar{\xi}(t)\}$.

B. *FEDNN Identification*

To generate a feasible reference trajectory, we employ a non-parametric identification scheme based on the Finite Element Differential Neural Network (FEDNN) framework established in [20]. Unlike traditional identifiers that treat the system as a black box, the FEDNN incorporates the spatial connectivity of the Finite Element Method (FEM) into the neural weight matrices.

Following the discretization described in equation (3), the dynamics of the 1D beam are approximated by the following neural structure:

$$\dot{\hat{x}}(t) = \Pi\hat{x}(t) + B\hat{W}(t)\Gamma(\hat{\Psi}(t)\hat{x}(t), U(t)) + L\Delta(t) \quad (6)$$

where $\hat{x} \in \mathbb{R}^{2N}$represents the estimated state (positions and velocities of the N nodes) and $B = \begin{bmatrix} 0 & I \end{bmatrix}^\top$. The matrix Π encodes the fixed connectivity of the beam elements composed as $\Pi = \begin{bmatrix} 0 & I \\ & A \end{bmatrix} \in \mathbb{R}^{2N\times 2N}$, the matrix $A \in \mathbb{R}^{N\times 2N}$ is composed of the mass (M), stiffness (K), and Rayleigh damping (D) matrices. Constructed through conventional FEM assembly procedures, these matrices depend on the beam's structural parameters, specifically the bending stiffness EI, $\Gamma(\Psi V(t), U(t)) =$

$\left[\sigma^\top(\Psi_1 V(t)) \quad (\phi(\Psi_2 V(t))U(t))^\top\right]^\top$ while $\hat{W}(t)$ and $\hat{\Psi}(t)$ are the adaptive weight matrices and L is an added matrix designed to ensure that $\Pi - L$ respect the Hurtwitz condition necessary for the identification.

The learning laws for $\hat{W}(t)$ and $\hat{\Psi}(t)$ are designed to ensure that the identification error $\Delta = x(t) - \hat{x}(t)$ remains uniformly ultimately bounded.

Following the Lyapunov stability analysis, the adaptive laws are given by:

$$\begin{aligned}\hat{W} &= -K_1^{-1}(I - \Lambda_\beta^{-1})^{-1}\Delta(t)^\top B^\top P\Gamma(\hat{\Psi}(t)\hat{x}(t), U(t))^\top \\ &\quad - \alpha_q(I + \Lambda_\beta^{-1})K_1\bar{W}(t) \\ \hat{\Psi} &= -K_2^{-1}(I - \Lambda_\alpha^{-1})^{-1}D^\top \overset{\circ}{W}^\top B^\top P\Delta(t)\hat{x}(t)^\top \\ &\quad - \frac{l}{2}\Lambda_4\bar{\Psi}(t)\hat{x}(t)\hat{x}(t)^\top - \alpha_q(I + \Lambda_\alpha^{-1})K_2\bar{\Psi}(t).\end{aligned} \tag{7}$$

Here, K_i, Λ_i are positive definite gain matrices of appropriate dimensions, and $\alpha_q > 0$. The matrix $P = P^\top > 0$ is the solution to the Algebraic Riccati Equation derived from the Lyapunov stability analysis. To handle the unknown ideal matrices W and Ψ, we propose nominal values derived from experimental data $\overset{\circ}{W}$ and $\overset{\circ}{\Psi}$, and define the error terms: $\overset{*}{W} = W - \overset{\circ}{W}$, $\overset{*}{\Psi} = \Psi - \overset{\circ}{\Psi}$, $\bar{W}(t) = \overset{\circ}{W} - \hat{W}(t)$, and $\bar{\Psi}(t) = \overset{\circ}{\Psi} - \hat{\Psi}(t)$.

We have formally proven that those learning laws guarantee that the identification error is exponentially ultimate bounded. Due to page constraints, the full stability proof is omitted; however, it follows from the Lyapunov candidate:

$$V(t) = |\Delta(t)|_P^2 + \mathrm{tr}\{\tilde{W}^\top K_1 \tilde{W}\} + \mathrm{tr}\{\tilde{\Psi}^\top K_2 \tilde{\Psi}\} \tag{8}$$

where $\tilde{\Psi} = \bar{\Psi} + \overset{*}{\Psi}$ and $\tilde{W} = \bar{W} + \overset{*}{W}$.

Making the generated trajectory $\hat{x}$ a reliable "digital shadow" of the physical plant it can be used as a reference for the control loop, effectively mitigating model mismatching issues.

III. Adaptive Control Design for Disturbance Rejection

This section details the control architecture designed for active vibration suppression. The proposed Model Reference Adaptive Control (MRAC) strategy diverges from conventional tracking formulations by utilizing the FEDNN output as a disturbance-free virtual reference. Consequently, the control objective shifts from following an arbitrary external command to rejecting the persistent perturbations acting on the plant. The specific modifications to the MRAC structure, including the design of the regressor vector, are presented first. Additionally, a Sliding Mode Control (SMC) approach in which as a reference the FEDNN model is used, is included as an alternative method, and serves as a comparison. The mathematical derivation of this controller is presented in Subsection III-B, providing the theoretical basis for the numerical validation discussed in Section IV.

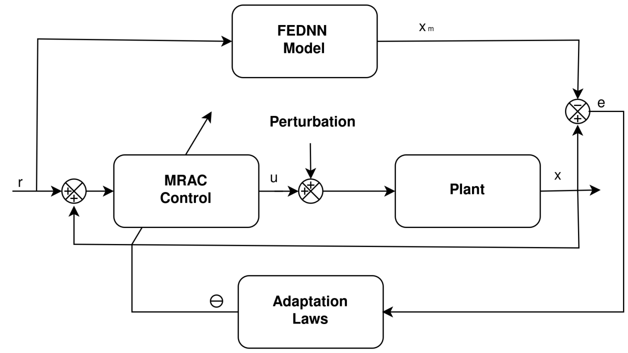

Fig. 2: Block diagram of the proposed nodal MRAC architecture. The diagram illustrates the closed-loop interaction between the reference model and the adaptive mechanism updating the controller gains.

A. MRAC Strategy

Once the feasible reference trajectory is generated by the FEDNN, the reference states $x_m(t)$ are compared to the plant states. The control objective is to force the plant states $x(t)$ to track $x_m(t)$ asymptotically, while simultaneously rejecting the persistent external disturbance $\xi(t)$. To achieve this, we propose a direct Model Reference Adaptive Control (MRAC) law.

We assume that the disturbance $\xi(t)$ is composed of bounded harmonic components. Consequently, the control law is structured not only to stabilize the plant, but also to counteract these specific frequency components. The proposed control input $u(t)$ is given by:

$$u(t) = K_x x + k_r r - \Theta(t)^\top \Phi(x), \tag{9}$$

where $\Theta(t) \in R^K$ is the vector of adaptive parameters, and $\Phi(x) \in R^K$ is the regressor vector. The matrices K_x and k_r can be calculated through the relations between the plant (A, B) and the reference model (A_m, B_m): $A + BK_x = A_m, Bk_r = B_m$. For this paper we consider a zero reference r in order to focus only in perturbation rejection.

To ensure effective rejection of the perturbation observed in the system, $\Phi(x)$ is constructed as a composite vector containing both the system state feedback and a set of harmonic basis functions:

$$\Phi(x) = [\sin(x_1(t)), \cos(x_2(t)), \dots]^\top. \tag{10}$$

This augmentation allows the adaptive controller to span the subspace of the disturbance, effectively canceling its effect on the tracking error.

To derive the adaptation mechanism, we define the tracking error as $e(t) = x(t) - x_m(t)$. The stability analysis is conducted using the Lyapunov candidate function as demonstrated in [3]:

$$V(e, \tilde{\Theta}) = e^\top Pe + \tilde{\Theta}^\top \Gamma^{-1}\tilde{\Theta}, \tag{11}$$

where $\tilde{\Theta}(t) = \Theta(t) - \Theta^*$ represents the parameter estimation error with respect to the ideal weights Θ^*. The matrix $\Gamma =$

$\Gamma^\top > 0$ determines the learning rate, and $P = P^\top > 0$ is the unique solution to the Lyapunov algebraic equation:

$$PA_m + A_m^\top P = -Q, \tag{12}$$

for a chosen positive definite matrix Q. Taking the time derivative of (11) along the error dynamics trajectories, the adaptation law that ensures $\dot{V} \le 0$ is derived as:

$$\dot{\Theta}(t) = -\Gamma\Phi(x)B^\top Pe(t). \tag{13}$$

Under this law, assuming the ideal case where the disturbance lies entirely within the span of the regressor basis $\Phi(x)$, the time derivative becomes $\dot{V} = -e^\top Qe \le 0$, guaranteeing asymptotic convergence to zero via Barbalat's Lemma.

However, in practical scenarios where $\xi(t)$ may contain unstructured components or higher-order harmonics not explicitly included in $\Phi(x)$, perfect cancellation is not theoretically guaranteed. Instead, the adaptation mechanism minimizes the projection of the disturbance onto the chosen basis. Consequently, the tracking error $e(t)$ is expected to converge to a small bounded residual set Ω_e rather than absolute zero. This behavior implies that the adaptive gains $\Theta(t)$ synthesize the best possible approximation of the required control effort to mitigate the dominant frequency components of the disturbance.

For a comprehensive overview of the proposed architecture, the complete block diagram illustrating the interaction between the FEDNN reference generator, the control strategy, and the flexible beam under disturbance is depicted in Fig. 2.

B. Sliding Mode Controller

To evaluate the proposed MRAC scheme against a robust distributed control benchmark, a Neural-Sliding Mode Control (NSMC) strategy is implemented based on the formulation by Poznyak [21]. Unlike the point-actuation limitation of the MRAC, this strategy assumes a distributed actuation capability to fully compensate for nonlinearities across the beam.

The control law is designed to enforce sliding modes on the error surface $s(t) = \Lambda^\top e(t) = 0$. In order to reject a perturbation $\xi(x,t)$, we incorporate the matrices obtained in the FEDNN identification, and as a digital shadow for the state, in order to follow a reference of how the system must behave without a perturbation. The control law is proposed as:

$$u_{nsmc}(t) = u_{eq}(t) + [W_2(t)\phi(\hat{x}(t))]u_{sw}(t), \tag{14}$$

where $u_{eq}(t)$ is a linearization of the system that use the adapted weights found through the FEDNN. So that:

$$u_{eq}(t) = [W_2\phi(\hat{x})]^+(\varphi(x_t^*, t) - A\hat{x} - W_1\sigma(\hat{x})) \tag{15}$$

where W_1 and W_2 denote the weight matrices of the trained neural network, while $\phi(\hat{x})$ and $\sigma(\hat{x})$ represent the sigmoid activation functions dependent on the FEDNN states ($\hat{x}$). The term $\varphi(x_t^*, t)$ corresponds to the desired trajectory generated by the nonlinear reference model (FEDNN). Finally, the matrix A is constructed as detailed in Section II-B.

The $u_{sw}(t)$ incorporates the sliding surface in order to cancel the negative influence of the perturbation and is defined as:

$$u_{sw}(t) = -kP^{-1}sign(\Delta_t) \tag{16}$$

where $k > 0$, $\Delta_t = x(t) - \hat{x}(t)$.

The schematic representation of the overall control system implementation is presented in Fig. 3.

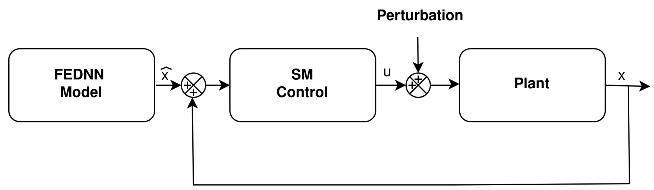

Fig. 3: Block diagram of the proposed NSM architecture. The diagram shows the utilization of the FEDNN model in the control loop.

IV. NUMERICAL VALIDATION

The numerical validation was designed to assess the robustness of the system model identified via experimental MoCap data (see Fig. 1) against persistent disturbances. A non-vanishing sinusoidal perturbation is introduced at $t = 13s$ at only one node. Unlike the impulse response in the open-loop experiment, this disturbance remains active throughout the simulation. Subsequently, at $t = 30$ s, the control loop is closed—activating either the MRAC or the Sliding Mode controller—to evaluate the vibration suppression capability. Crucially, the control input is applied to a different node than the disturbance, testing the effectiveness of the scheme in a non-collocated scenario.

A. Vibration Suppression Performance

The tracking performance of both control strategies is illustrated in Fig. 4.

As observed in Fig. 4b, the distributed Neuro Sliding-Mode Control (NSMC) reacts faster, reducing the perturbation almost instantaneously due to its high-gain switching nature and multi-node actuation. In contrast, the proposed MRAC (Fig. 4a) exhibits a brief transient adaptation phase. Once the adaptive gains $\Theta(t)$ tune to the frequency of the disturbance, the vibration is effectively depleted.

As illustrated in Fig. 4b, the NSMC drives the system to a stable state almost immediately due to its robust nature. However, it is observed that the tracking error does not vanish completely but remains bounded within a narrow region around zero. This 'quasi-sliding' behavior is attributed to the finite switching frequency of the digital implementation (chattering) and the residual approximation error of

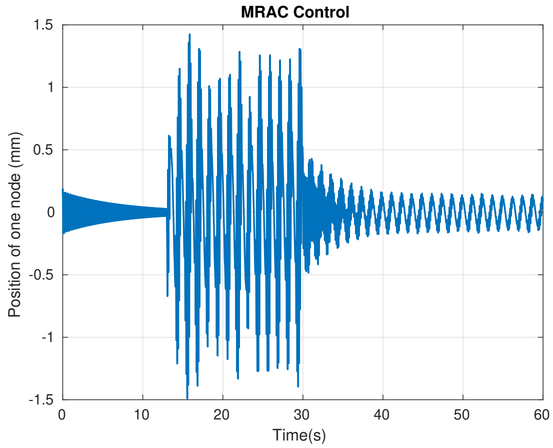

(a)

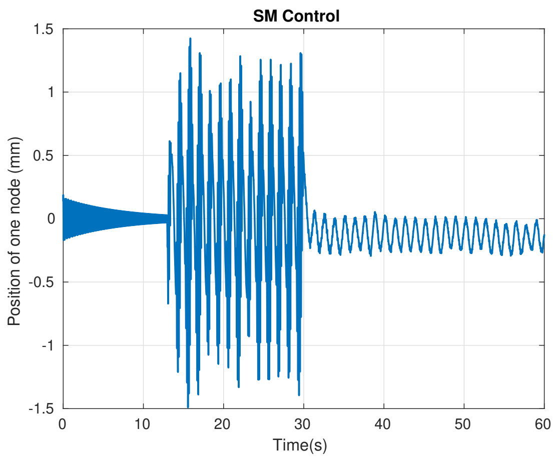

(b)

Fig. 4: Comparative time evolution of the displacement at the beam's free tip (last node). (a) Response using the proposed FEDNN-MRAC. (b) Response using the distributed Neural-Sliding Mode Control (NSMC).

the neural component, which prevents perfect asymptotic convergence to the sliding manifold.

It is noteworthy that despite the MRAC acting on a single node (non-collocated configuration), it achieves a steady-state error convergence comparable to the distributed NSMC. This validates the fact that the augmented regressor $\Phi(t)$ successfully captures the internal model of the disturbance.

B. Control Effort

While the tracking errors are similar, a critical disparity appears when analyzing the control signals $u(t)$ required by each strategy, as shown in Fig. 5.

The NSMC signal (Fig. 5b) displays the characteristic high-frequency chattering caused by the signum function in the sliding mode law. Although effective for robustness, this discontinuous switching demands excessive bandwidth from the actuators and can induce mechanical wear or heating in practical piezoelectric applications.

Conversely, the proposed FEDNN-MRAC generates a smooth, continuous control signal (Fig. 5a). The adaptive mechanism synthesizes a counter-acting sinusoidal wave that precisely cancels the external disturbance. This "smooth modulation" implies significantly lower energy consumption and falls well within the physical bandwidth constraints of standard actuators. Consequently, the MRAC approach offers a superior trade-off between vibration suppression accuracy and hardware feasibility.

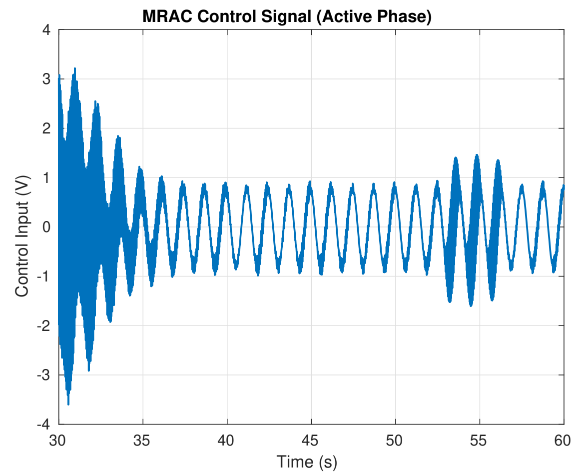

(a)

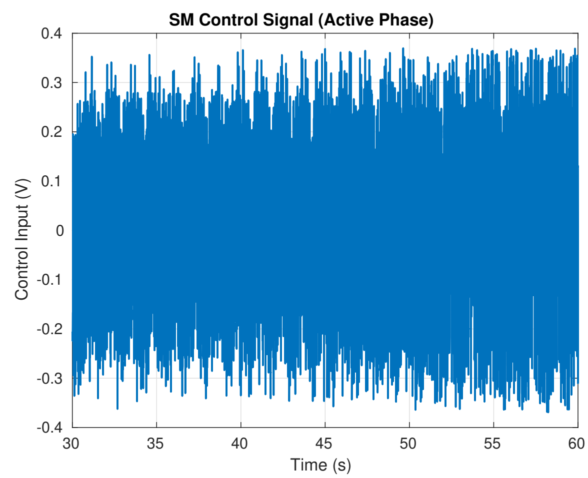

(b)

Fig. 5: Time evolution of the control effort $u(t)$ required for disturbance attenuation. (a) Control signal of the FEDNN-MRAC strategy. (b) Control signal of the NSMC strategy.

While only the sinusoidal case is illustrated for brevity, the architecture was validated across multiple harmonic disturbances with consistent results, as summarized in Table I.

TABLE I: Quantitative Performance Comparison

Strategy	**RMSE** (mm)	t_s (s)	**ISC** (V^2s)
NSMC	0.1603	< 1	22.8307
MRAC	0.1058	4.5	17.3459

V. Discussion and Future Work

The numerical validation presented in this study demonstrates that both the distributed Neural-Sliding Mode Control (NSMC) and the proposed nodal FEDNN-MRAC are capable of rejecting non-vanishing matched perturbations in flexible structures. However, a detailed inspection of the results reveals critical operational trade-offs that determine the suitability of each approach for practical implementations.

In the case of the FEDNN-MRAC, a residual oscillation arises because the regressor basis $\Phi(x)$ is a finite approximation; it cannot perfectly cancel harmonic components or unmodeled dynamics that fall outside its span.

Conversely, the residual error in the NSMC is primarily a consequence of the chattering phenomenon. Since ideal infinite switching is impossible in numerical implementation, the state trajectory becomes trapped within a small boundary layer around the sliding manifold $s = 0$. Furthermore, the approximation error inherent to the neural component of the sliding law contributes to this bounded steady-state error.

Regarding performance, the NSMC exhibits a shorter settling time, driving the error to a bounded region near zero almost immediately after activation. Nevertheless, this robustness comes at a high implementation cost: it assumes a fully distributed actuation capability (actuators at every node) and generates a control signal characterized by high-frequency switching (chattering). This "chaotic" behavior, visible as a dense band in the control plot, implies extreme acceleration demands that can lead to actuator saturation or mechanical fatigue in real-world scenarios.

In contrast, the proposed FEDNN-MRAC achieves effective vibration suppression using a single point actuator (non-collocated configuration). Although the settling time is slightly longer due to the adaptation transient, the generated control signal is smooth and continuous, resembling a counter-acting harmonic wave. While the error does not converge to absolute zero—exhibiting a small residual oscillation around the equilibrium—this is an expected consequence of the approximation error in the neural reference and the steady-state ripple of the adaptive gains. The key finding is that the MRAC provides a feasible engineering solution with significantly reduced hardware complexity compared to the distributed sliding mode baseline.

Real-world constraints include actuator response lags and the current MoCap setup, which do not yet allow for online closed-loop control. Nevertheless, FEDNN-based control remains computationally efficient as complexity is shifted to the offline identification phase, ensuring lightweight real-time inference.

Future work will focus on three main avenues: (i) the derivation of a point-actuated Sliding Mode strategy to enable a fairer comparison considering under-actuated conditions; (ii) an optimization analysis to determine the ideal sensor-actuator pair placement along the beam that minimizes the residual MRAC error; and (iii) the refinement of the regressor vector $\Phi(x)$ or the inclusion of an integral term to achieve perfect asymptotic regulation (zero steady-state error) rather than bounded stability.

Acknowledgment

The first author (A. Diaz) was supported by the Mexican National Council of Science, Humanities, Technology and Innovation (SECIHTI).

References

[1] D. Zhang and B. Wei, "A review on model reference adaptive control of robotic manipulators," *Annual Reviews in Control*, vol. 43, pp. 188–198, 2017.

[2] S. Djebbri, S. Ladaci, A. Metatla, and H. Balaska, "Fractional-order model reference adaptive control of a multi-source renewable energy system with coupled dc/dc converters power compensation," *Energy Systems*, vol. 11, no. 2, pp. 315–355, 2020.

[3] N. T. Nguyen, "Model-reference adaptive control," in *Model-Reference Adaptive Control: A Primer*. Springer, 2018, pp. 83–123.

[4] K. Rui, G. Wenjun, and C. Yunxia, "Model-driven degradation modeling approaches: Investigation and review," *Chinese Journal of Aeronautics*, vol. 33, no. 4, pp. 1137–1153, 2020.

[5] V. I. Utkin and I. Vadim, "Sliding mode control," *Variable structure systems: from principles to implementation*, vol. 66, no. 1, 2004.

[6] Y. Shtessel, C. Edwards, L. Fridman, A. Levant *et al.*, *Sliding mode control and observation*. Springer, 2014, vol. 10.

[7] K. David Young and Ü. Özgüner, "Frequency shaping compensator design for sliding mode," *International Journal of Control*, vol. 57, no. 5, pp. 1005–1019, 1993.

[8] W. He and J. Liu, *Active vibration control and stability analysis of flexible beam systems*. Springer, 2019.

[9] R. S. Sutton, A. G. Barto, and R. J. Williams, "Reinforcement learning is direct adaptive optimal control," *IEEE control systems magazine*, vol. 12, no. 2, pp. 19–22, 2002.

[10] L. Buşoniu, T. De Bruin, D. Tolić, J. Kober, and I. Palunko, "Reinforcement learning for control: Performance, stability, and deep approximators," *Annual Reviews in Control*, vol. 46, pp. 8–28, 2018.

[11] B. Ma, Z. Liu, Q. Dang, W. Zhao, J. Wang, Y. Cheng, and Z. Yuan, "Deep reinforcement learning of uav tracking control under wind disturbances environments," *IEEE Transactions on Instrumentation and Measurement*, vol. 72, pp. 1–13, 2023.

[12] F. Z. Kadri, R. G. Hadiby, K. Boumediene, Y. Derkaoui, B. Daaou, and A. Djellouli, "Model reference adaptive control based on neural network for depth of an auv," *Journal of Maritime Research*, vol. 22, no. 1, pp. 146–154, 2025.

[13] F. Guo, F. Wang, Y. Qin, and Y. Mei, "Adaptive neural network vibration control for a flexible vehicle-based arm with input-state constraints," *Transactions of the Institute of Measurement and Control*, p. 01423312251388188, 2025.

[14] Q. Song, S. Li, Q. Bai, J. Yang, A. Zhang, X. Zhang, and L. Zhe, "Trajectory planning of robot manipulator based on rbf neural network," *Entropy*, vol. 23, no. 9, p. 1207, 2021.

[15] E. Kökçam and N. Tan, "Comparison of adaptation mechanisms on mrac," *IEEE Access*, vol. 12, pp. 31 862–31 874, 2024.

[16] K.-Y. Hu, W. Sun, and C. Yang, "Adaptive fault-tolerant control for flexible variable structure spacecraft with actuator saturation and multiple faults," *Applied Sciences*, vol. 12, no. 11, p. 5319, 2022.

[17] C. Kong, D. Zhao, and B. Liang, "Vibration suppression of a flexible beam structure coupled with liquid sloshing via adp control based on fbg strain measurement," in *Actuators*, vol. 12, no. 12. MDPI, 2023, p. 471.

[18] W. He, T. Meng, S. Zhang, J.-K. Liu, G. Li, and C. Sun, "Dual-loop adaptive iterative learning control for a timoshenko beam with output constraint and input backlash," *IEEE Transactions on Systems, Man, and Cybernetics: Systems*, vol. 49, no. 5, pp. 1027–1038, 2017.

[19] Y. W. Kwon and H. Bang, *The finite element method using MATLAB*. CRC press, 2018.

[20] O. Aguilar-Leal, R. Q. Fuentes-Aguilar, I. Chairez, A. García-González, and J. C. Huegel, "Distributed parameter system identification using finite element differential neural networks," *Applied Soft Computing*, vol. 43, pp. 633–642, 2016.

[21] A. S. Poznyak, E. N. Sanchez, and W. Yu, *Differential neural networks for robust nonlinear control: identification, state estimation and trajectory tracking*. World Scientific, 2001.